SUPPLEMENTARY INFORMATION

The AMPK-related kinase NUAK2 affects tumor growth, migration and clinical outcome of human melanoma

Takeshi Namiki, Atsushi Tanemura, Julio C. Valencia, Sergio C. Coelho, Thierry Passeron, Masakazu Kawaguchi, Wilfred D. Vieira, Masashi Ishikawa, Wataru Nishijima, Toshiyuki Izumo, Yasuhiko Kaneko, Ichiro Katayama, Yuji Yamaguchi, Lanlan Yin, Eric C. Polley, Hongfang Liu, Yutaka Kawakami, Yoshinobu Eishi, Eishi Takahashi, Hiroo Yokozeki and Vincent J. Hearing

Experimental Procedures

Tumor specimens. We obtained 92 paraffin-embedded specimens of primary melanomas from 3 institutions. This study was approved by the Tokyo Medical and Dental University Research Committee, the Osaka University Clinical Research Committee and the Saitama Cancer Center Research Ethics Committee. Fifty-seven tumors were classified as acral melanomas and 35 as non-CSD melanomas according to the definition by Curtin and colleagues (1). The clinical features of these cases are summarized in SI Table 4.

Cell lines. Normal human melanocyte and melanoma cell lines were cultured and maintained as previously described (2). Melanoma cell lines used were C32, A375, A2058, Malme-3M, SKMel5, SKMel28, SKMel23, 586mel, mel2 and mel18. C32, A375, A2058, and Malme-3M cells were purchased from the American Type Culture Collection. SKMel5, SKMel28, SKMel23 and 586mel cells were kindly provided by the Surgery Branch, NCI/NIH, Bethesda, MD. mel2 and mel18 melanoma cells are as previously described (3).

Statistical analyses of a public database. CGH array data of primary melanomas were obtained from Series “GSE2631” (http://www.ncbi.nlm.nih.gov/geo/) (1). Clones with a log2 ratio value more than 0.25 were classified as “gain” (4). Chromosomal loci were estimated as “gained” when log2 values of 3 clones among 4 consecutive clones were more than 0.25. Genomic clones were estimated as “gained” when log2 value of the corresponding clone was more than 0.25. Genomic areas between 2 adjacent clones were also estimated as “gained” when log2 values of the 2 adjacent clones were more than 0.25 at the same time. Genomic clones were estimated as “deleted” when log2 value of the corresponding clone was less than -0.4. Correlations between each chromosomal gain, gain of each clone and tumor thickness were analyzed by the Mann-Whitney test. The threshold of statistical significance was adjusted to p-value of 0.0071 by multiple corrections.

Quantitation of DNA copy numbers and mRNA expression levels. Analyses of DNA copy numbers and mRNA expression levels by quantitative real time PCR were performed using a LightCycler 480 Real-Time PCR System. Quantitative real-time PCR was performed using a LightCycler 480 SYBR Green I Master kit (Roche Applied Systems). The DNA copy number of each candidate gene was quantified by comparing the target locus to the reference Line-1 element as previously described (5). The cDNA level (mRNA expression level) of each candidate gene was quantified by comparison with the cDNA level of 18S RNA. PCRs for each primer set were performed at least in triplicate. Human genomic DNA was used as a calibrator for DNA copy number analyses and the cDNA of HEMn-DP was used as a calibrator for mRNA expression level analyses. Conditions for PCR reactions were as follows: 1 cycle at 95°C for 10 min, 40 cycles at 95°C for 10 s, at 55°C for 12 s, and at 72°C for 10 s. Melting curve analyses confirmed that single products were amplified and agarose gel electrophoresis

was also carried out to confirm that PCR products were of the predicted lengths. Primer sequences for each target used in the DNA copy number analyses are as follows: ***SOX13*** forward 5-ATTGGTTGAGGACCATGTGC-3 and reverse 5-GCGAGCTGTCTCTCTCCAAA-3; ***MDM4*** forward 5-TGTGTAAAGGCCTGGGTAGG-3 and reverse 5-AACCTCTAACTGCCCAGCAA-3; ***NUAK2*** forward 5-CACCCTTGCAGAGATGATGA-3 and reverse 5-CCAGGGAATTGGATACATGG-3; ***ELK4*** forward 5-CAGCTGCCCCAGATTTTATT-3 and reverse 5-GAATCTCAAATTGCCTTTGTCA-3; ***IKBKE*** forward 5-TTTGGCCATAAAACCTGACC-3 and reverse 5-AGCAGGGCATCAACTCCTAA-3; ***MAPKAPK2*** forward 5-CCAGTCCCGAGACACTCTGT-3 and reverse 5-GGCAGAAGCACCAGGTTAAA-3. Primer sequences for each target used in the mRNA expression level analyses are as follows: ***SOX13*** forward 5-AAGGATGAGCGGAGGAAGAT-3 and reverse 5-CTCCTGGTTGGTCATGGACT-3; ***MDM4*** forward 5-GGTGGAGATCTTTTGGGAGAA-3 and reverse 5-AGCAGTGGCTAAAGTGACAAGA-3; ***NUAK2*** forward 5-GTCAATCCGGAAGGACAAAA-3 and reverse 5-TCACGATCTTGCTGCTGTTC-3; ***ELK4*** forward 5-AGCCGAGCCCTCAGATACTA-3 and reverse 5-CACAGTCACCCTCAATCCTG-3; ***IKBKE*** forward 5-GACCAGTTCTTTGCGGAGAC-3 and reverse 5-GCCTCCTGGAAAATGGCTA-3; ***MAPKAPK2*** forward 5-GAAGTGCCTGCTGATTGTCA-3 and reverse 5-CGATGCTCTTCATGATTTCG-3. Quantification of DNA copy number and cDNA level was performed by comparison with standard curves generated from dilution series of human genomic DNA and cDNA of HEMn-DP. DNA copy numbers and mRNA expression levels of candidate genes were automatically calculated using the LightCycler480 Relative Quantification software.

Vectors, siRNA transfection and Lentiviral infection. SMARTpool siRNAs against NUAK2, ELK4 and MAPKAPK2 were purchased from Dharmacon. Lentiviral vectors carrying shRNA targeting NUAK2 (AAB66-F-6: AAACCCAGGGCTGCCTTGGAAAAG and AAB66-F-7: AAACCCAGGGCTGCCTTGGAAAAG) and the empty vector were purchased from Open Biosystems in pLKO.1puro vector. For siRNA experiments, cells were seeded at 2.0 x 10^5 cells/well in 6-well plates and were transfected either with an siNT (non-targeting) or with an siRNA against NUAK2, ELK4 or MAPKAPK2 (SMARTpool siRNAs, Dharmacon) at a concentration of 100 pmol/well using Lipofectamine RNAiMAX (Invitrogen) according to the manufacturer's protocol. All siRNA experiments were performed in triplicate. Lentivirus containing shRNA constructs with pLKO.1 against NUAK2 were produced in NCI-Frederick and C32, mel2, mel18, A375, SKMel28 and SKMel23 melanoma cells were infected using protamine sulfate. Infected cells were then selected by puromycin. The knockdown of NUAK2 expression was confirmed at the mRNA level by real-time PCR analyses.

In Vitro Assays. For cell number analyses using siRNA, cells were seeded at 2.0 x 10^5 cells/well in 6-well plates in triplicate. Cell numbers were counted at 72 h after transfection of siRNA and statistical differences between siNT and the siRNA against each candidate gene were calculated. For cell number analyses using shRNA, cells were seeded at 1.0 x 10^5 cells/well in 6-well plates in triplicate. Counting of cell numbers were started (as day 0) after 72 h selection with puromycin. Cell numbers were counted at days 0, 3, 6 and 9.

For cell cycle profile and apoptosis analysis, cells were stained with a solution containing 0.1% Triton X-100, 0.1% Na citrate and 50 μg/ml propidium iodide (PI), and then were analyzed using an FACSCalibur (BD). Percentages of cells in G0/G1, S, G2/M and pre-G1 phases were calculated with CellQuest Pro software (BD).

For the wound healing assay, scratches were made in confluent C32 melanoma cell monolayers grown in ImageLock 24-well plates using a Woundmaker (Essen). Cells were placed in an IncuCyte (Essen) and the wounds were imaged every 2 hr for 48 hr. The percent wound closure after 48 hr was determined using IncuCyte scratch wound assay software (Essen).

For the migration assay, the BD Falcon FluoroBlok 24-Multiwell Insert System was used. Cells were seeded at $5x10^4$ cells/well in 24-well plates in triplicate and were labeled with calcein AM (Invitrogen). OD values were counted at 36 h after seeding using a 1420 Multilabel Counter Victor3 (Perkin Elmer). Migration of C32 melanoma cells infected with the empty vector (shEV) was set at 100%, and cell counts were adjusted by the difference between the proliferation of C32 melanoma cells infected with shEV or shNUAK2 at 36 h. SA-β-gal staining was performed using a Senescence β-Galactosidase Staining Kit according to the manufacturer's protocol (Cell Signaling).

Animal model. All animal experiments were approved by the NCI-Bethesda Animal Care and Use Committee of the National Cancer Institute. One week after infection of lentiviruses and selection using puromycin, 2.0×10^6 C32 melanoma cells (infected with shEV or shNUAK2) were injected subcutaneously into nude mice (4 or 5 per group as noted). Mice were then monitored for tumor appearance and tumor sizes were measured until day 40 or until the tumor measured 2 cm in diameter.

Immunoblotting. Immunoblotting was performed as previously described (2). Antibodies used included a rabbit polyclonal antibody to NUAK2 (1:1000, Proteintech Group), a mouse monoclonal antibody to actin (1:1000; Abcam), a mouse monoclonal antibody to cdc2 (1:1000; Santa Cruz Biotechnology), a rabbit polyclonal antibody to CDK2 (1:1000; Santa Cruz Biotechnology), a mouse monoclonal antibody to CDK4 (1:1000; Cell Signaling), a mouse monoclonal antibody to CDK6 (1:500; Abcam), a rabbit monoclonal antibody to cyclin D1 (1:1000; Cell Signaling), a mouse monoclonal antibody to cyclin D3 (1:2000; Cell Signaling), a mouse monoclonal antibody to cyclin E (1:500; Abcam), a rabbit monoclonal antibody to caspase-3 (1:5000; Cell Signaling), a rabbit polyclonal antibody to cleaved PARP (1:1000; Cell Signaling), a rabbit monoclonal antibody to mTOR (1:1000; Cell Signaling) and a rabbit polyclonal antibody to Rheb (1:1000; Cell Signaling).

Immunohistochemical analysis. Formalin-fixed, paraffin-embedded tissues on slides were deparaffinized by 2 washes, 5 min each, with xylene. Tissues were rehydrated by a series of 3 min washes in 100%, 95%, 70%, 50% ethanol and a 5 min wash in distilled water. Antigen retrieval was performed by heating the slides at 95°C for 15 to 30 min in Antigen Unmasking Solution (Vector Laboratories). Endogenous peroxidase activity was blocked by treatment with 3% H_2O_2 for 15 min. After blocking with normal horse serum (Vector Laboratories) for 30 min, the tissues were incubated with a rabbit polyclonal anti-NUAK2 antibody (1:100, Proteintech Group) at 4°C overnight. The tissues were then incubated with a biotin-labeled secondary antibody and then with avidin-peroxidase for 30 min each (Vector Laboratories). The slides were then developed with a Vector VIP Substrate Kit (Vector Laboratories) and were counterstained with HematoxylinQS (Vector Laboratories). The slides were then dehydrated following a standard procedure, and sealed with coverslips.

Confirmation of the specificities of antibodies was carried out using a lentivirus carrying an shRNA targeting NUAK2 (for the antibody against NUAK2) (SI Fig. 7A). Immunostaining was scored from 0 to +3 (0 = 0 to10%, +1 =11% to 25%, +2 = 26% to 50% or +3 = 51% to 100%) in a blind fashion by 3 observers using positive cells in eccrine and in sebaceous glands as internal positive controls (SI Fig. 7B). The basal expression group (negative staining group) includes specimens with a 0 score and the high expression group (positive staining group) includes specimens with +1, +2 or +3 scores.

Statistical analysis. Regression analysis was used to test the association between DNA copy number and mRNA expression level of each candidate gene. Student's *t* test was used to explore the difference of cell numbers between the NUAK2 knockdown group and the control group. The Chi square test was employed to test the association between NUAK2 expression and two clinical parameters: gender and

ulceration. The Mann-Whitney test was used to evaluate the correlation between expression level of NUAK2 and the other two clinical parameters, tumor thickness and age. The Kaplan-Meier method and log-rank test were used to evaluate the difference of patient survival between the NUAK2-positive group and the NUAK2-negative group The Cox regression model was applied to investigate the effect of NUAK2 expression on clinical survival of melanoma patients. Time dependent sensitivity and specificity of the binary classifier were calculated by R package SurvivalROC (6, 7). Statistical analyses were performed in R and SAS.

Supplemental Figures

SI Fig. 1. Knockdown of NUAK2, ELK4 and MAPKAPK2 using siRNA SMARTpools. Immuno-blotting showing knockdown of NUAK2, ELK4 and MAPKAPK2 at 24, 48 and 72 h after siRNA transfection. An siRNA Non-targeting pool was used as a control (siNT).

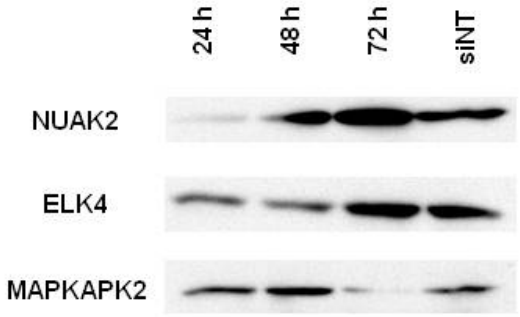

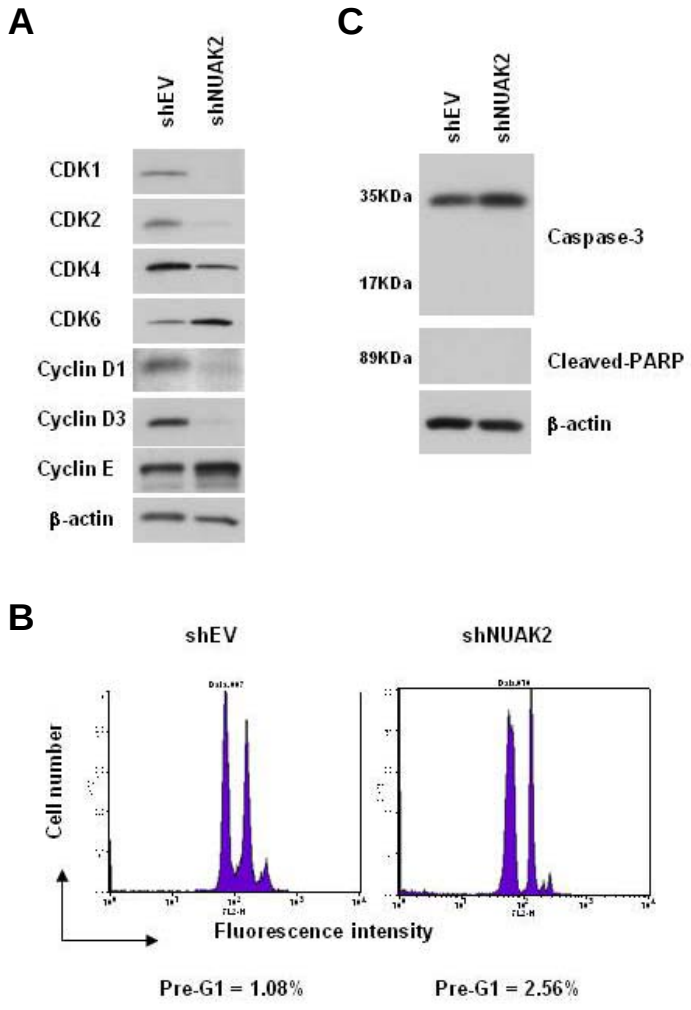

SI Fig. 2. Knockdown of NUAK2 in C32 melanoma cells and apoptosis. (**A**) Immunoblotting showing the expression of CDK1, CDK2, CDK4, CDK6, cyclinD1, cyclinD3 and cyclinE. β-actin was used as a loading control. Knockdown of NUAK2 decreases cyclinD1, cyclinD3, CDK1 and CDK2 expression level in C32 melanoma cells. **(B)** Knockdown of NUAK2 has a slight effect on the pre-G1 phase population of cells. **(C)** Immunoblotting shows no cleaved caspase-3 or PARP with knockdown of NUAK2 in C32 melanoma cells.

SI Fig. 3. Migration assays with knockdown of NUAK2 using C32 melanoma cells. (**A**) Migration of C32 melanoma cells with knockdown of NUAK2 using a wound healing assay. Images at 0, 24h, 36h and 48h after scratch are shown. Upper and lower panels of each time point show wound healing assays using C32 melanoma cells infected with a lentivirus carrying an empty vector (shEV) and an shRNA targeting NUAK2 (shNUAK2), respectively. **(B)** Migration of C32 melanoma cells with knockdown of NUAK2 using the FluoroBlok system. Knockdown of NUAK2 significantly decreased the migration of C32 melanoma cells; the P value is indicated.

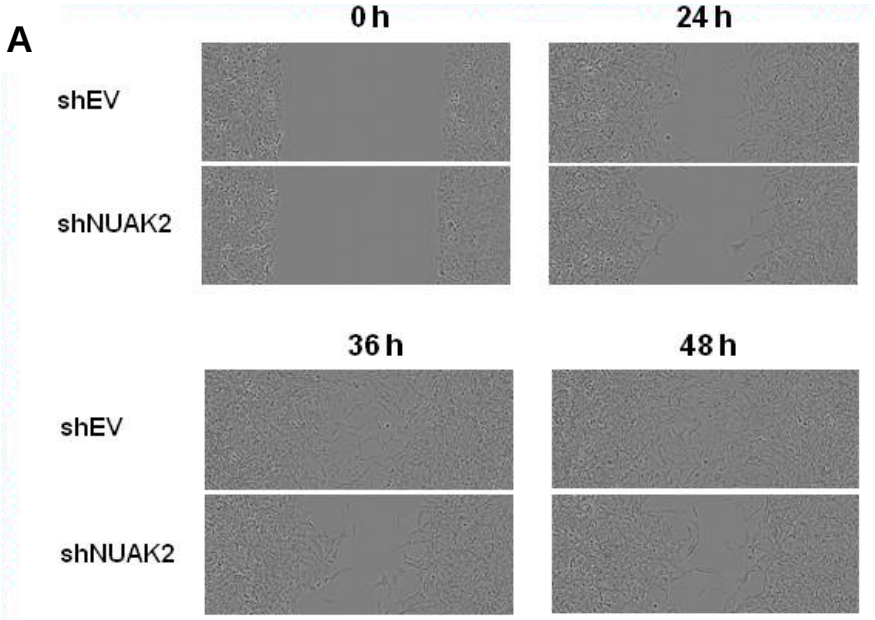

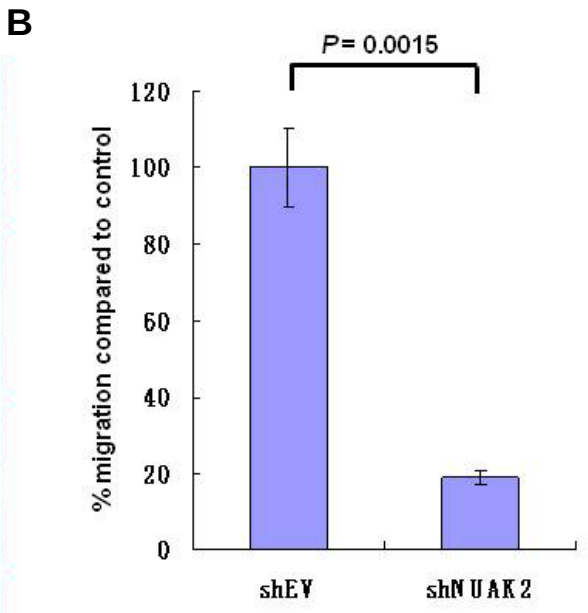

SI Fig. 4. Knockdown of NUAK2 in various melanoma cell lines and apoptosis. (**A**) Immunoblotting shows expression of NUAK2 in various melanoma cell lines. (**B**) Knockdown of NUAK2 has a marked effect on the pre-G1 phase population in mel18 and in SKMel28 melanoma cells and a slight effect in mel2 and in SKMel23 melanoma cells.

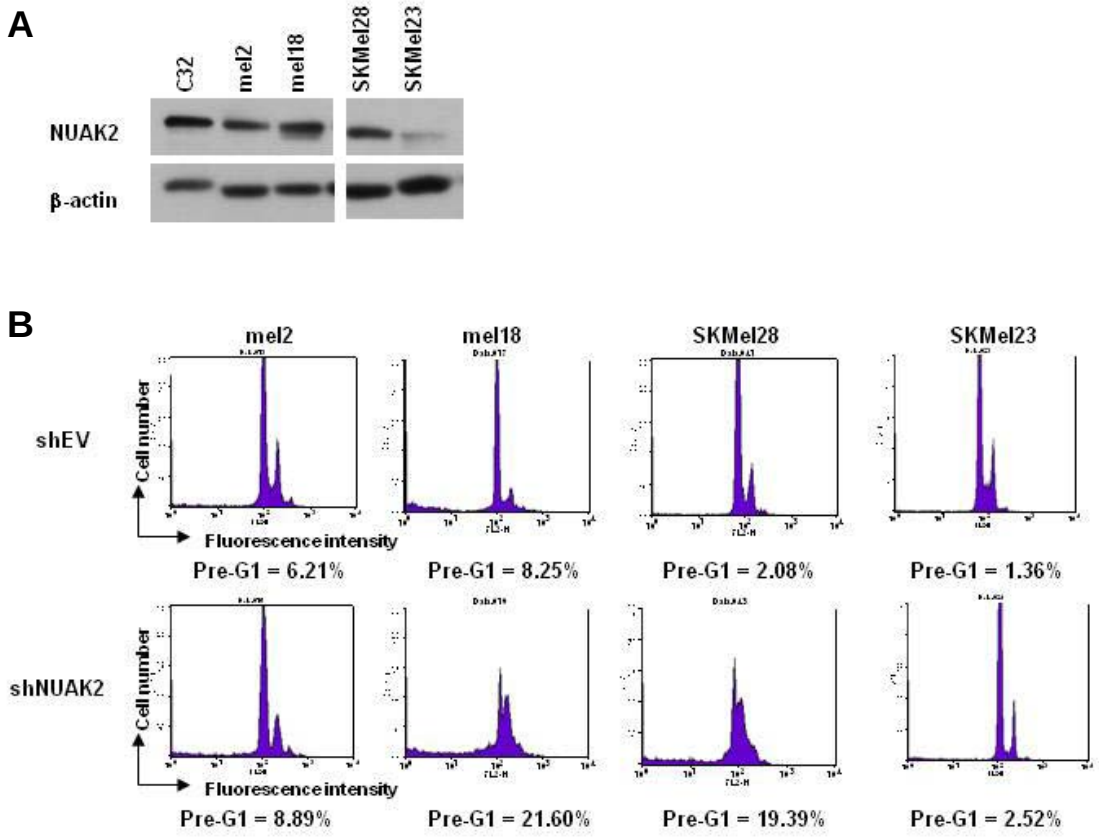

SI Fig. 5. Immunohistochemical analyses of NUAK2 expression in clinical specimens. (A) NUAK2 was highly-expressed in the acral melanoma of case No. 23 and that staining was counted as strong (+3) (left panel). NUAK2 was not expressed in the acral melanoma of case No. 24 and that staining was counted as negative (0) (middle panel). NUAK2 was not expressed in the non-CSD melanoma of case No. 60, and that staining was counted as (0) (right panel). (**B**) NUAK2 expression and H&E staining of case No. 26. The image with low magnification at the bottom shows both the radial growth phase (right portion) and the vertical growth phase (left portion). The insets above show higher magnification images (X10) of areas indicated by arrows. Each upper inset shows NUAK2 staining and each lower inset shows H&E staining; insets on the right show melanoma cells in the epidermal portion. Individual melanoma cells, which are forming tumor nests in the lower epidermis, express high levels of NUAK2; insets on the left show that melanoma cells form nests and invade into the deep dermis, and also express NUAK2 at significant levels. Bar indicates 1 mm.

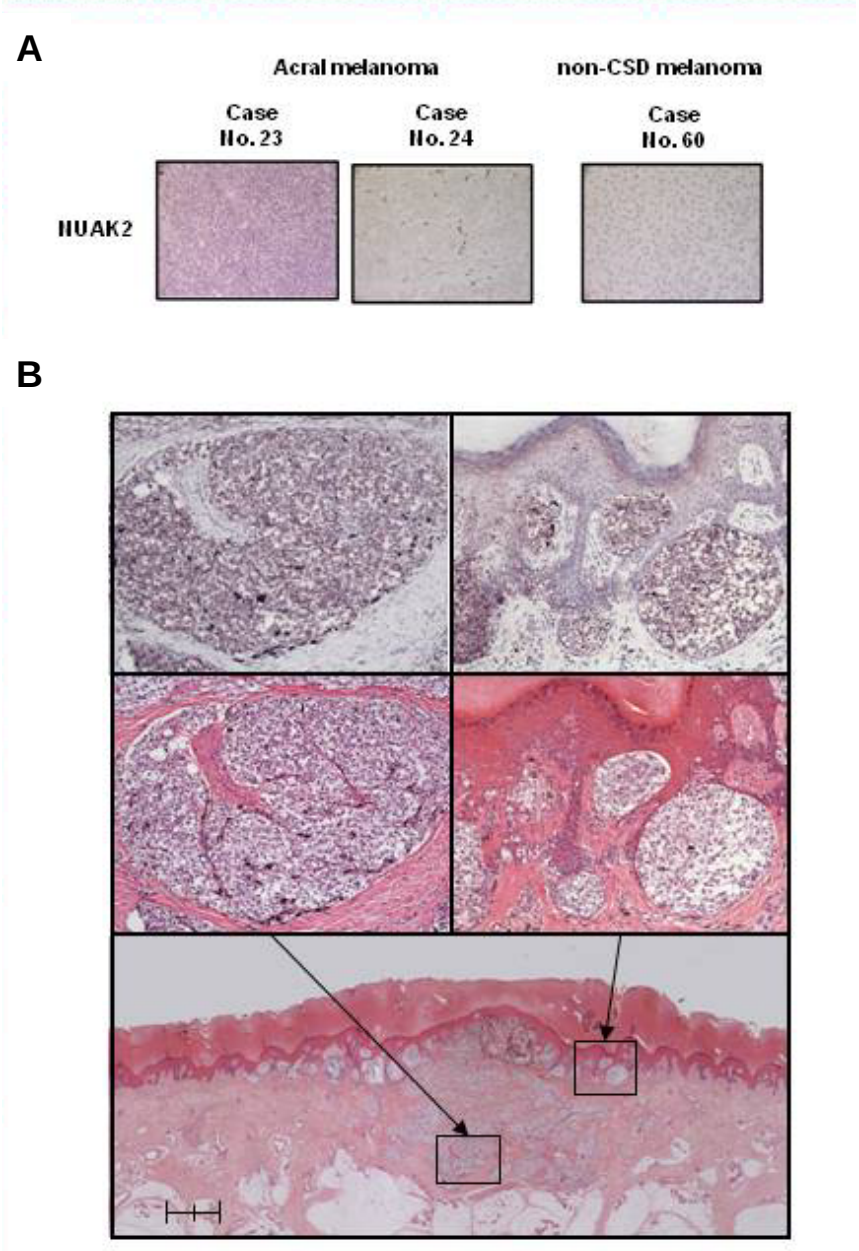

SI Fig. 6. Survival analyses of high expression levels of NUAK2 in the pTis+pT1/pT2+pT3 and pT4 stages of acral melanomas. Kaplan-Meier survival analyses of high expression levels of NUAK2 for relapse-free survival of 34 cases in the pTis+pT1 and pT2+pT3 stages (left) and of 23 cases in the pT4 stage of acral melanomas (right); P values are indicated in all graphs.

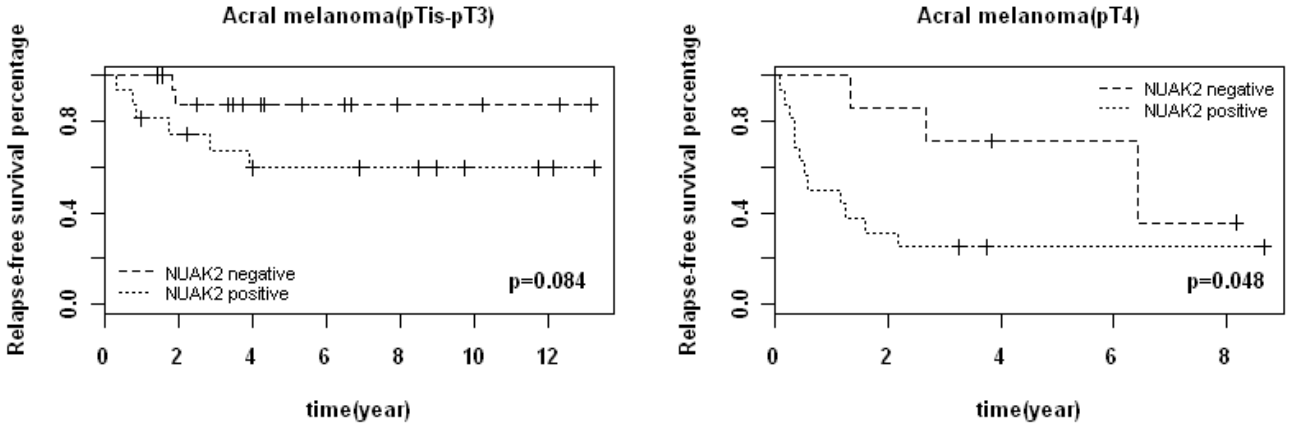

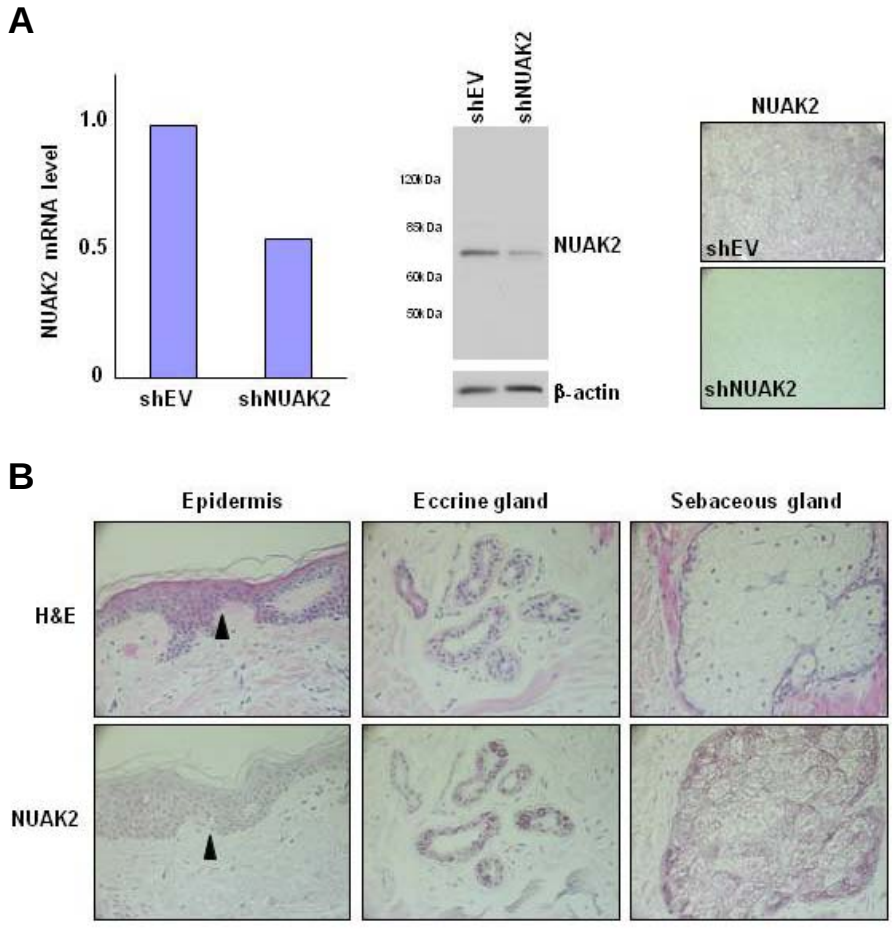

SI Fig. 7. Specificity of the NUAK2 antibody and the staining pattern of NUAK2 in normal skin. (A) Specificity of the NUAK2 antibody. Real time PCR analysis shows the specific knockdown of NUAK2 expression using a lentivirus carrying an shRNA targeting NUAK2 (shNUAK2) at the mRNA level; an empty vector (shEV) was used as the control (left). Immunoblotting (middle) and immunohistochemical analysis (right) shows the knockdown of NUAK2 expression in shNUAK2-infected cells; this result was obtained in 2 of 4 experiments. **(B)** Staining pattern of NUAK2 antibody in normal skin. Negative staining of keratinocytes and melanocytes in normal epidermis is shown (arrowheads indicate melanocytes). Strong staining was observed both in dark and in clear cells of eccrine glands and in sebaceous cells of sebaceous glands.

Supplemental Tables

SI Table 1. Comparison of tumor thickness and each chromosomal gain.

	Acral	Non-CSD	CSD	Mucosal	All
1q21-23	$P = 0.06$	$P = 0.26$	$P = 0.46$	$P = 0.86$	$P = 0.0053^{**}$
1q32	$P = 0.017^{*}$	$P = 0.54$	$P = 0.71$	NA	$P = 0.003^{**}$
6p23-25	$P = 0.29$	$P = 0.98$	$P = 0.093$	$P = 0.70$	$P = 0.10$
6p21	$P = 0.043$	$P = 0.39$	$P > 0.99$	$P = 0.0068^{***}$	$P = 0.087$

$^{*}P < 0.05$; $^{**}P < 0.01$;*** inverse correlation

SI Table 2. Comparison of tumor thickness and each genomic clone.

Clone ID	Acral	Non-CSD	CSD	Mucosal	All
RP11-154A22	$P = 0.56$	NA	NA	$P = 0.46$	$P = 0.32$
RP11-249C10	$P = 0.36$	$P > 0.99$	$P = 0.54$	$P = 0.71$	$P = 0.15$
RP11-150L7	$P = 0.054$	$P = 0.74$	$P = 0.91$	NA	$P = 0.0051^{**}$
RP11-246J15	$P = 0.024^{*}$	$P = 0.33$	$P = 0.79$	NA	$P = 0.023$
RP11-65I22	$P = 0.013^{*}$	$P = 0.80$	$P = 0.33$	NA	$P = 0.0034^{**}$
RP11-148K15	$P = 0.94$	$P = 0.49$	$P > 0.99$	$P > 0.99$	$P = 0.72$
RP11-243M13	$P = 0.0029^{**}$	$P = 0.43$	$P = 0.14$	NA	$P = 0.0004^{**}$
RP11-249H15	$P = 0.47$	$P = 0.78$	$P = 0.37$	NA	$P = 0.94$
RP11-219P13	$P = 0.08$	$P = 0.45$	$P = 0.36$	$P = 0.38$	$P = 0.0098^{*}$
RP11-57I17	$P = 0.30$	$P = 0.36$	$P = 0.85$	$P = 0.28$	$P = 0.03^{*}$
RP11-45F21	$P = 0.27$	$P = 0.22$	$P = 0.67$	$P = 0.071$	$P = 0.092$
RP11-167J2	$P = 0.72$	$P = 0.47$	$P = 0.44$	$P = 0.64$	$P = 0.053$
RP11-104A2	$P = 0.52$	$P = 0.97$	$P = 0.70$	$P = 0.13$	$P = 0.42$

SI Table 3. DNA copy number and mRNA expression of candidate genes at 1q32 by real-time PCR analyses.

DNA copy number

	C32	A375	A2058	Malme-3M	SKMel5	SKMel28	SKMel23	568mel	mel2	mel18
SOX13	3.44	1.36	1.76	1.78	1.72	1.09	1.32	2.31	2.14	1.12
MDM4	3.95	1.62	1.82	1.87	2.01	1.29	0.86	2.85	2.14	1.02
NUAK2	3.94	1.73	2.15	2.13	2.21	1.42	1.33	2.69	2.75	1.65
ELK4	5.73	2.05	2.89	2.45	2.34	1.43	0.91	2.74	1.68	1.13
IKBKE	3.72	1.48	1.99	1.79	1.46	1.18	0.83	2.37	2.01	1.22
MAPKAPK2	1.10	1.26	1.83	1.65	1.38	1.08	0.93	2.40	2.39	1.39

mRNA expression

	C32	A375	A2058	Malme-3M	SKMel5	SKMel28	SKMel23	568mel	mel2	mel18
SOX13	2.75	0.37	0.34	0.88	0.22	1.35	0.17	1.31	0.83	1.50
MDM4	1.59	1.19	1.12	0.79	1.41	0.68	0.74	1.60	3.18	1.64
NUAK2	4.55	1.11	1.14	0.98	1.66	0.78	1.07	2.26	1.70	0.55
ELK4	1.80	0.78	0.66	0.97	1.14	0.83	0.44	1.99	1.33	0.63
IKBKE	0.34	0.75	1.30	0.76	0.61	0.42	0.59	1.48	1.15	0.55
MAPKAPK2	0.86	0.67	1.34	0.88	0.48	0.74	0.43	1.55	1.15	0.53

Acral melanoma

Case No	Age/ Sex	Tumor Thickness	TNM classification	Clinical Stage	Present Status	RS	OS	NUAK2
1	71F	14.0mm	pT4bN3M0	IIIC	DOD	5	8	+2
2	57M	9.4mm	pT4bN3M0	IIIC	CCR	45+	45+	+2
3	90M	4.5mm	pT4bN3M0	IIIC	DOD	7	15	+3
4	66M	8.1mm	pT4bN2bM0	IIIC	CCR	104+	104+	+3
5	86M	1.8mm	pT2aN2bM0	IIIB	CR-R	4	13+	+3
6	70M	8.2mm	pT4bN2aM0	IIIB	CR-R-CR	19	39+	+3
7	56M	7.0mm	pT4bN2aM0	IIIB	DOD	6	13	+3
8	79F	7.0mm	pT4aN1bM0	IIIB	DOD	15	74	+2
9	58M	0.8mm	pT1aN2aM0	IIIA	DOD	22	89	0
10	63M	8.0mm	pT4aN1aM0	IIIA	DOD	16	17	0
11	23F	1.8mm	pT2aN1aM0	IIIA	CCR	141+	141+	+2
12	70M	19.0mm	pT4bN0M0	IIC	DOD	2	6	+2
13	79M	15.0mm	pT4bN0M0	IIC	DOD	4	5	+3
14	75F	10.0mm	pT4bN0M0	IIC	CCR	3	100+	+2
15	65F	9.0mm	pT4bN0M0	IIC	DOD	26	37	+1
16	52M	6.5mm	pT4bN0M0	IIC	CCR	46+	46+	0
17	51M	5.5mm	pT4bN0M0	IIC	CCR	98+	98+	0
18	55M	5.0mm	pT4bN0M0	IIC	DOD	1	17	+3
19	79F	5.0mm	pT4bN0M0	IIC	CCR	46+	46+	0
20	78M	4.7mm	pT4bN0M0	IIC	CCR	39+	39+	+2
21	80F	4.5mm	pT4bN0M0	IIC	DOD	4	5	+3
22	79M	4.2mm	pT4bN0M0	IIC	CCR	32+	32+	0
23	66M	4.1mm	pT4bN0M0	IIC	CCR	39+	39+	+3
24	54M	10.0mm	pT4aN0M0	IIB	CCR	32	138+	0
25	49F	5.5mm	pT4aN0M0	IIB	DOD	77	82	0
26	78M	4.2mm	pT4aN0M0	IIB	CR-R	14	31+	+3
27	57M	3.2mm	pT3bN0M0	IIB	CCR	117+	117+	+3
28	66M	2.4mm	pT3aN0M0	IIA	CCR	64+	64+	0
29	76F	2.2mm	pT3aN0M0	IIA	CCR	10	88+	+3
30	68F	2.1mm	pT3aN0M0	IIA	CCR	108+	108+	+1
31	71M	2.1mm	pT3aN0M0	IIA	CCR	102+	102+	+2
32	74F	2.1mm	pT3aN0M0	IIA	CCR	146+	146+	+3
33	71M	1.6mm	pT2bN0M0	IIA	CCR	30+	30+	0
34	37F	1.6mm	pT2bN0M0	IIA	DOD	47	63	+1
35	54M	1.5mm	pT2bN0M0	IIA	CR-R	34	51+	+1
36	54M	1.5mm	pT2bN0M0	IIA	CCR	83+	83+	+1
37	68F	1.8mm	pT2aN0M0	IB	CCR	21	61	+2
38	84F	1.8mm	pT2aN0M0	IB	DOD	9	23	+2
39	66F	1.7mm	pT2aN0M0	IB	CCR	148+	148+	0
40	56F	1.3mm	pT2aN0M0	IB	CCR	95+	95+	0
41	76F	1.2mm	pT2aN0M0	IB	CCR	42+	42+	0
42	54F	1.2mm	pT2aN0M0	IB	CCR	17+	17+	0
43	58F	1.2mm	pT2aN0M0	IB	CCR	48+	48+	+2
44	36M	0.7mm	pT1bN0M0	IB	CCR	123+	123+	0
45	73F	0.9mm	pT1aN0M0	IA	CCR	80+	80+	0
46	57M	0.9mm	pT1aN0M0	IA	CCR	51+	51+	0
47	79F	0.8mm	pT1aN0M0	IA	CCR	12+	12+	+1
48	70F	0.8mm	pT1aN0M0	IA	CCR	159+	159+	+1
49	52F	0.5mm	pT1aN0M0	IA	DOD	23	37	0
50	76F	0.4mm	pT1aN0M0	IA	CCR	78+	78+	0
51	77M	0.4mm	pT1aN0M0	IA	CCR	52+	52+	0
52	49F	0.5mm	pTisN0M0	0	CCR	158+	158+	0
53	63M	0.5mm	pTisN0M0	0	CCR	30+	30+	0
54	62M	0.5mm	pTisN0M0	0	CCR	45+	45+	0
55	77F	0.3mm	pTisN0M0	0	CCR	40+	40+	0
56	62F	0.3mm	pTisN0M0	0	CCR	19+	19+	0
57	49F	0.3mm	pTisN0M0	0	CCR	27+	27+	+2

Non-CSD melanoma

Case No	Age/ Sex	Tumor Thickness	TNM classification	Clinical Stage	Present Status	RS	OS	NUAK2
58	91F	6.0mm	pT4bN3M0	IIIC	DOD	4	10	+2
59	64F	2.6mm	pT3aN3M0	IIIC	DOD	5	14	+2
60	49M	12.0mm	pT4bN2bM0	IIIC	CR-R	8	13+	0
61	69M	6.3mm	pT4bN2bM0	IIIC	DOD	26	30	+3
62	64F	9.2mm	pT4bN1bM0	IIIC	DOD	2	35	+1
63	40M	8.0mm	pT4bN2cM0	IIIB	CCR	62+	62+	0
64	56F	10.0mm	pT4aN2bM0	IIIB	CR-R	24	28+	0
65	50F	3.5mm	pT3aN1bM0	IIIB	CR-R	64	147+	0
66	70M	3.5mm	pT3aN1bM0	IIIB	CR-R	64	147+	+3
67	28F	9.5mm	pT4bN1aM0	IIIB	CCR	45+	45+	+2
68	60F	3.8mm	pT3bN1aM0	IIIB	CR-R-CR	52	97+	0
69	59F	2.1mm	pT3aN2aM0	IIIA	CR-R	16	23+	+3
70	28F	6.5mm	pT4aN1aM0	IIIA	DOD	60	62	+2
71	42M	3.8mm	pT3aN1aM0	IIIA	DOD	54	69	+2
72	53M	6.0mm	pT4bN0M0	IIC	CCR	66+	66+	0
73	78F	5.0mm	pT4bN0M0	IIC	CCR	36+	36+	0
74	66M	3.0mm	pT3bN0M0	IIB	DOD	58	96	0
75	40M	3.0mm	pT3bN0M0	IIB	CCR	124+	124+	+1
76	55M	3.3mm	pT3aN0M0	IIA	CCR	135+	135+	+3
77	24M	2.5mm	pT3aN0M0	IIA	DOD	76	79	+3
78	32F	2.2mm	pT3aN0M0	IIA	CCR	60+	60+	+3
79	58F	2.0mm	pT3aN0M0	IIA	CR-R	17	25+	0
80	36M	1.8mm	pT2aN0M0	IB	CCR	43+	43+	+3
81	58F	1.5mm	pT2aN0M0	IB	CR-R	31	36+	+2
82	19F	1.3mm	pT2aN0M0	IB	CCR	47+	47+	+2
83	41F	1.2mm	pT2aN0M0	IB	CCR	78+	78+	+3
84	55F	1.2mm	pT2aN0M0	IB	CCR	45+	45+	+3
85	63F	2.0mm	pT1bN0M0	IB	CR-R	52	73+	0
86	48F	1.0mm	pT1aN0M0	IA	CR-R	9	26+	0
87	50F	0.8mm	pT1aN0M0	IA	CCR	38+	38+	0
88	62M	0.5mm	pT1aN0M0	IA	CCR	12+	12+	+2
89	37F	0.5mm	pT1aN0M0	IA	CCR	12+	12+	+2
90	36F	0.5mm	pTisN0M0	0	CCR	180+	180+	+2
91	37M	0.3mm	pTisN0M0	0	CCR	41+	41+	0
92	30F	0.3mm	pTisN0M0	0	CCR	51+	51+	0

SI Table 4. Clinical parameters, expression of NUAK2, and survival information for 57 acral and 35 non-CSD melanomas.

TNM classification and clinical stage are according to the melanoma staging system of the American Joint Committee on Cancer. Expression of NUAK2 is estimated with 4 histopathological scores of 0, +1, +2 and +3. A + after survival indicates that the patient is alive.

Abbreviations: **DOD**, died of disease; **CCR**, continuous complete remission; **CR-R**, complete remission followed by relapse; **CR-R-CR**, complete remission followed by relapse and subsequent complete remission; **RS**, relapse free survival; **OS**, overall survival

SI Table 5. Correlations of clinical parameters with high expression levels of NUAK2.

	Acral melanoma	Non-CSD melanoma
Thickness	$P = 0.0026$**	$P = 0.71$
Sex	$P > 0.99$	$P > 0.99$
Ulceration	$P = 0.017$*	$P = 0.15$
Age	$P = 0.088$	$P = 0.43$

*$P < 0.05$; **$P < 0.01$

SI Table 6. Sensitivity and specificity of using NUAK2 expression status to predict relapse of acral melanoma at 3 time points.

Time point	2 yrs	3 yrs	4 yrs
sensitivity	0.829	0.797	0.802
specificity	0.565	0.585	0.607

SI References

1. Curtin JA *et al.* (2005) Distinct sets of genetic alterations in melanoma *New Eng J Med* 353, 2135-2147.
2. Watabe H *et al.* (2004) Regulation of tyrosinase processing and trafficking by organellar pH and by proteasome activity *J Biol Chem* 279, 7971-7981.
3. Ashida A, Takata, M., Murata, H., Kido, K. & Saida, T. (2009) Pathological activation of KIT in metastatic tumors of acral and mucosal melanomas *Int J Cancer* 124, 862-868.
4. Fridlyand J, Snijders, A. M., Pinkel, D., Albertson, D. G. & Jain, A. N. (2004) Hidden Markov models approach to the analysis of array CGH data *J Multivar Anal* 90, 132-153.
5. Zhao X *et al.* (2004) An integrated view of copy number and allelic alterations in the cancer genome using single nucleotide polymorphism arrays *Cancer Res* 64, 3060-3071.
6. Heagerty PJ, Lumley, T. & Pepe, M. S. (2000) Time-dependent ROC curves for censored survival data and a diagnostic marker *Biometrics* 56, 337-344.
7. Heagerty PJ & Zheng, Y. (2005) Survival model predictive accuracy and ROC curves *Biometrics* 61, 92-105.